POLISH JOURNAL OF SOIL SCIENCE
VOL. LIV/1 2021 PL ISSN 0079-2985

DOI: 10.17951/pjss/2021.54.1.1

AMAR KUMAR KATHWAS*, NILANCHAL PATEL*

GEOMORPHIC CONTROL ON SOIL EROSION – A CASE STUDY IN THE SUBARNAREKHA BASIN, INDIA

Received: 09.04.2020
Accepted: 17.02.2021

Abstract. Geomorphology depicts the qualitative and quantitative characteristics of both terrain and landscape features combined with the processes responsible for its evolution. Soil erosion by water involves processes, which removes soil particles and organic matter from the upper sheet of the soil surface, and then transports the eroded material to distant location under the action of water. Very few studies have been conducted on the nature and dynamics of soil erosion in the different geomorphologic features. In the present investigation, an attempt has been made to assess the control of geomorphologic features on the soil loss. Universal Soil Loss Equation (USLE) was used to determine soil loss from the various geomorphological landforms. Principal component analysis (PCA) was implemented on the USLE parameters to determine the degree of association between the individual principal components and the USLE-derived soil loss. Results obtained from the investigation signify the influence of the various landforms on soil erosion. PC5 is found to be significantly correlated with the USLE-derived soil loss. The results ascertained significant association between the soil loss and geomorphological landforms, and therefore, suitable strategies can be implemented to alleviate soil loss in the individual landforms.

Keywords: geomorphological feature, soil erosion, USLE, principal component analysis

* Department of Remote Sensing, Birla Institute of Technology, Mesra, Ranchi, Jharkhand, India. Pin: 835215. Corresponding author: nilanchal.patel@gmail.com

INTRODUCTION

The landform is a broad classification of planetary landscape structures based on its shape. Landforms create terrain and their arrangement in a landscape is termed as "topography"(Mukherjee *et al*. 2013, Pennock 2003). Prolonged phenomena of weathering and erosion along with the tectonic activities have resulted in different types of configuration of the landforms. Both during and after their formation, the landforms become susceptible to weathering and erosion of different intensities owing to the variation of five dominant controlling factors such as topography (slope and relief), parent rock material, structural features (faults, folds, joints, etc.), weathering and eroding agents (running water, glacier and wind), and climate. Therefore, each landform manifests strong bearing of the various influencing factors that have led to its present disposition. In view of the prevalence of the various interrelated processes as mentioned above, the various landforms can be broadly categorized as erosional, denudational and depositional.

Several researchers have studied the relationship between landforms and land cover. Mainuri and Owino (2014) performed investigation to link landforms and landuse with land degradation. Abdel Rahman *et al.* (2018) quantified the suitability of land units for horticultural and field crops in the different landform units. Segundo *et al.* (2017) explored the quantitative relation between the landforms and different land covers. McGrath *et al*. (2011) examined the impact of interactions between the eco-hydrological process on the geomorphology and spatial organization of vegetation cover. The results show that the feedback between the vegetation patterns and soil have significant amount of influence on the changing topography. Saco *et al*. (2007), using a coupled dynamic vegetation-landform evolution model, performed an investigation to explore the interactions between the vegetation pattern and landform evolution. The study suggests that interaction between the vegetation and erosion tends to modify the micro topography, which subsequently alters the landcover pattern.

The complex feedback system between the landforms and land cover, significantly influences soil erosion. The influence of the natural factors, viz. precipitation, soil, parent rock material, topography, slope, relief, elevation, climate, land covers, drainage pattern, etc. on the soil erosion process is well recognized and studied, worldwide (Marston 2010, Patel and Kathwas 2012, Patton *et al*. 2018, Pelletier *et al*. 2013, Schoonover and Crim 2015), whereas few researchers attempted to explore the influence of the geomorphic structures on the soil erosion process. Earth surface processes such as erosion by water shape, are influenced by the topography (Champagnac *et al*. 2012, Whipple 2009), and subsequently, landforms. Soil erosion process disrupts soil aggregates and the soil's structural stability leading to reduced water holding capacity, nutrient reserve and thereby reducing plant productivity on eroding landform posi-

tions. Geomorphologists have recognized a strong connection between the slope morphology and erosion rates (Morgan and Nearing 2016, Morgan and Rickson 2003). Conoscenti *et al*. (2008) performed geomorphological study to evaluate the water erosion susceptibility using a geostatistical multivariate approach.

Natural soil erosion by the energy of wind, raindrops, or running water accelerates by almost every human use of landscapes: agriculture, grazing, and timber harvesting (Council 2010, Wischmeier and Smith 1978). Therefore, understanding the influence of geomorphology of landscape and its associated processes is vital for the conservation and sustainability of the environment. In the backdrop of the complex association between the geomorphology and surface process, it is pertinent to carry out quantitative appraisal of soil erosion in terms of geomorphology, as a spatial unit of assessment. In order to accomplish the desired objectives, universal soil loss equation (USLE), developed by the Agricultural Research Service (ARS) scientists Wischmeier and Smith (1978), was used for the soil loss estimation from the individual landform units. The equation integrates the effect of five prominent erosion-governing parameters, namely rainfall erosivity (R), soil erodibility (K), topography (LS), crop management (C) and, the conservation practice (P). The results of the present research will be insightful in the holistic characterization of the erosional and/or depositional attributes of each landform unit.

OBJECTIVES OF THE INVESTIGATION

The primary aim of the present investigation is to assess the influence of landforms on the soil erosion intensity. The sub-objectives of the investigation comprise an assessment of the:

- spatial distribution pattern of the soil erosional severity zones in the different landform units,
- degree of association between the principal components developed using the USLE factors as inputs and erosional intensity corresponding to the individual landforms,
- relationship between the computed principal components and the USLE factors corresponding to the individual landforms and,
- difference between the mean erosional intensities of the different pairs of landform units employing Welch's *t*-test. The analysis was performed for 170 pairs of landforms.

MATERIALS AND METHODS

Study area

The study area (Fig. 1) selected for the present investigation lies in the southern part of the Jharkhand state, between 23°52' to 23°03' latitude and 85°16' to 85°86' longitude covering nearly 2,229 sq. km area. The relief of topography decreases from the west to east. Slope gradient varies from 0 to 50 degrees with the highest relief and steep slopes identified in the central portion of the study area. The western portions have elevation high above 750 m, whereas that of the eastern region has elevation of 180 m above the mean sea level. The study area comprises parts of the Subarnarekha river basin, which lies in the Chota Nagpur Plateau. The region is dissected by rivers of varying degree of magnitude flowing from the west to east. The study area experiences subtropical climate, which is characterized by hot summer from March to May with temperatures ranging between 20 to 40 degrees, and the winter season is pronounced by dry and cold weather during the month of November to February with temperatures varying from 0 to 25 degrees. The study area witnesses average rainfall of 1,400 mm, which is well distributed during southwest monsoon period from June to

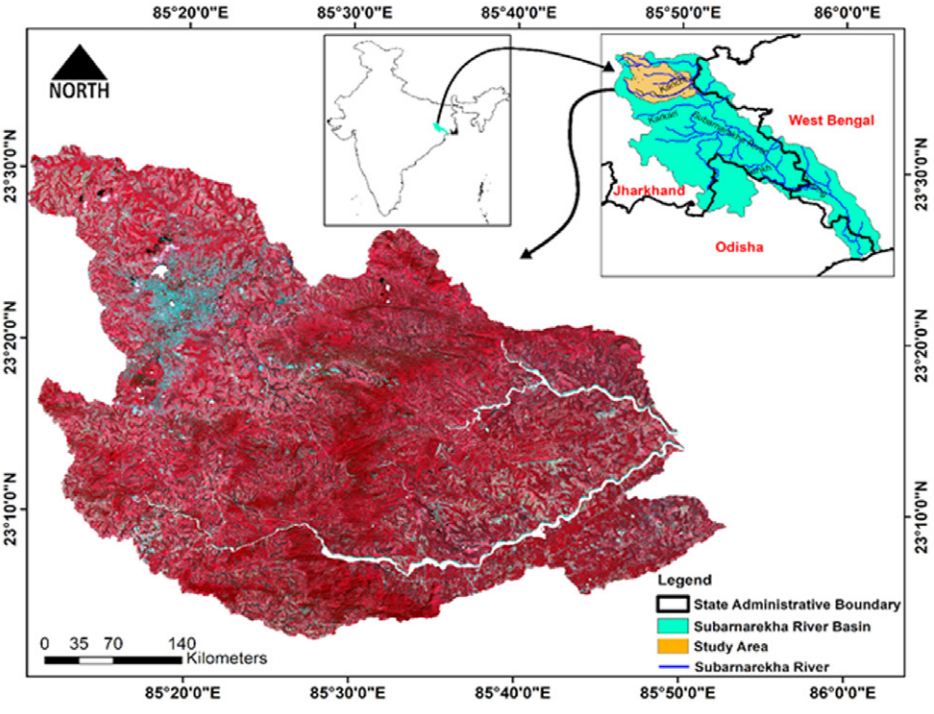

Fig. 1. Map showing the location of the study area

October. Agriculture is the dominant land use category, followed by natural vegetation cover. The northern and southern part of the study area is covered with hillocks and forest. The soils of the study area are mostly of the residual type. High temperature and high rainfall have led to the formation of lateritic type of soils from the rocks of Archean metamorphic complex. Texturally the soils can be classified into following classes: Stony and gravelly soils, Red and yellow soils, Lateritic soils, Alluvial soils.

Physical and geomorphic landforms present in the study area

The major landforms identified in the study area are grouped under three categories, namely (a) erosional (b) depositional and (c) denudational, and described as follows:

I. Erosional landforms

a) Structural hill: Structural hills are the geologic structures formed by the forces such as folding, faulting, bedding, joint, lineaments, etc. In the study area, structural hills cover 16.3% of the area and can be observed in the central part running from the north to south. The structure found in the study area is the resultant of faulting, which has also resulted in the upliftment of the western part compared to the east. It is believed to have undergone uplift as the side effects of the Himalayan orogeny, particularly during the late Tertiary period. Steep slopes on the hills can be observed, which may cause quicker erosion of the softer elements below the harder rocks at the lower end. Moreover, the structural hills of the study area comprise moderate to dense vegetation cover as the major land cover.

b) Plateau slightly/moderately dissected: A dissected plateau represents slightly to moderately eroded landform showing a sharp relief. Such an area may be referred to as mountainous, but dissected plateaus are distinguishable from the orogenic mountain belts by the lack of folding, metamorphism, extensive faulting, or magmatic activity that accompanies orogeny. Majority of the slightly dissected plateau can be found in the north central portion, while moderately dissected plateau can be observed in the south and south-central parts of the study area.

c) Valley: A valley is a low area between hills, often with a river running through it. In geology, it is termed as a depression that is longer than its width. The terms “U-shaped” and “V-shaped” are the descriptive terms of geography to characterize the different genesis of valleys. The features cover 6.2% of the area and can be observed in the northwest and south-west portion of the study area.

d) **Valley gullied:** A valley which is originally worn away by the running water and serving as a drainage way after prolonged heavy rains. These geomorphic features are formed by the action of Kanchi river water on the lower plateau region, in the south-eastern part of the study area. The landform occupies 2.5% of the total study area.

e) **Plateau weathered moderate/shallow:** These are shallow and moderate to highly fractured weathered surfaces. The surface of these geomorphic units is moderately dissected by the streams of rivers, giving rise to a terrain consisting of flat-topped ridges and steep scarps. It is a major geomorphic feature of the study area covering nearly 20.6 and 30.4% of the area and can be observed in the upper and lower regions of the study area, respectively.

f) **Pediment moderately dissected:** A pediment is a very gentle slope (5°–7°) inclined bedrock surface typically sloping down from the base of a steeper retreating cliff, or escarpment; but may continue to exist after the mountain has eroded away. It is caused by erosion, it develops when sheets of running water (laminar sheet flows) wash over it in intense rainfall events. Eroded by drainage and river channels of the study area, the geomorphic feature can be observed to a small extent in the southern part of the study area.

g) **Intermontane valley:** It is represented as a wide valley between the mountain ranges that is partly filled with alluvium. It is confined in the north-central portion of the study area. The underlying materials in these features are silt, clay, sand and alluvium. These features have fertile soils and better groundwater prospects.

II. Depositional landforms

a) **Valley fill shallow:** Valley fill is the fundamental landform produced by the lateral erosion associated with the bedrock erosion surfaces, which remains unidentified due to the commonly veneered alluvium. These geomorphic features differ in shapes and sizes and, in the beginning, it may accentuate the impression of a flood plain because of the covered alluvium. Valley fills can be found in the lower plateau region areas of Subarnarekha, Kanchi and Karkari river basin, in the east and south-east covering 4.2% of the total study area. The landform is marked with moderate to good cultivation and at some places is covered with vegetation cover.

b) **Piedmont slope:** It is a gentle slope leading from the base of a mountain to a region of flat land. These are formed by the lateral coalescence of a series of alluvial fans. Typically, it has broadly undulating transverse profile, parallel to the mountain front, resulting from the

convexities of the component fans. The term is generally restricted to the constructional slopes of intermontane basins.

c) **Lateritic plain moderate:** Tropical weathering (laterization) is a prolonged process of chemical weathering, which produces a wide variety in the thickness, grade, chemistry and ore mineralogy of the resulting soils. The features develop by intensive and long-lasting weathering of the underlying parent rock and are rich in iron and aluminum. It occurs in insignificant amount in the study area in the northern part of the upper plateau region.

d) **Pediplain shallow:** They are formed by the coalescence of buried pediments, where a thick overburden of weathered materials accumulates. The intensely weathered areas of granitoids constitute these landforms. Varying thickness of shallow overburden can be observed in such areas. Weathering of the bedrocks has been initiated by fractures, joints and minor lineaments. These can be found in the extreme south-east part of the study area covering only 0.5% of the study area.

e) **Alluvium sand silt dominant:** These are loose, unconsolidated soil or sediments (sand, silt), which get eroded, reshaped, and deposited around the banks of the river Kanchi.

III. Denudational landforms

a) **Pediment inselberg complex:** This complex consists of small isolated hills standing out prominently because of their resistance to weathering. The pediments dotted with a number of inselbergs, which cannot be separated and mapped as individual units are referred to as pediment inselbergs complex having moderate to steep slope. In the study area, the feature can be observed in the west and west-central region covering 5.2% of the area. These are controlled by structures like joints, fracture and lineaments.

b) **Denudational hill:** These landforms are represented as a group of massive hills with resistant rock bodies, formed due to different erosional and weathering processes. These features generally have poor groundwater potential, which results in dry and rough surface cover. The feature can be observed in the south-central part of the upper plateau region covering only 0.8% of the total study area.

c) **Residual hill:** The formation of these geomorphic features is controlled by joints and fractures, and is generally represented as a group of hills, occupying comparatively smaller area than a composite hill. These hard rocks left behind after erosion can be found in the west, south-west and north eastern parts of the study area, and cover only 0.8% of the total study area.

d) **Inselberg:** These are isolated rock hill, knob, ridge, or small mountains that rise abruptly from a gently sloping or virtually level surrounding plain. The landform includes conical hills with rectilinear sides typically found in arid regions; regolith-covered concave-convex hills; rock crests over regolith slopes; rock domes with near vertical sides; tors (koppies) formed of large boulders but with solid rock cores. These features cover 0.2% of the total study area, scattered all around and dome-shaped, formed from granite or gneiss. They can also be called "bornhardt", though all bornhardts are not inselbergs.

e) **Hilltop weathered:** Hilltop weathered come in many shapes, but most have an area of relatively much gentle slope or flat ground. Many hill tops, particularly in an area or very old landscapes, have the extensive area of flat ground (hill top weathered). The features can be found in the central portion of the study area and are primarily covered with dense vegetation cover.

f) **Inselberg complex:** These comprise more than one isolated low relief hill, which occur close to each other. These features occur in the north-central region of the study area and cover insignificant part.

The geomorphological landform map of the study area is shown in Fig. 2.

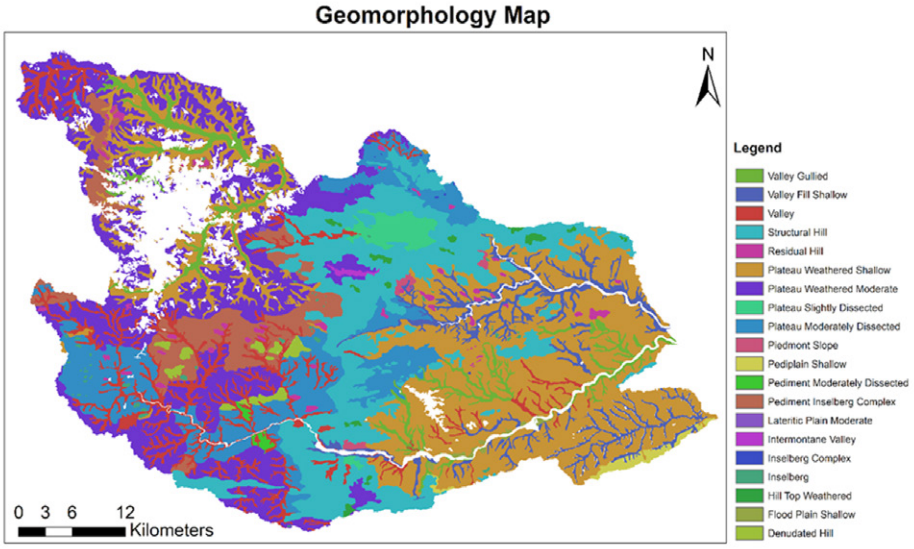

Fig. 2. Geomporphological landforms in the study area

At the outset, satellite imageries pertaining to the Landsat 8 Operational Land Imager (OLI) (30 meters), ASTER GDEM (30 meters), and Climatologies at High Resolution for the Earth's Land Surface Areas (CHELSA) Precipita-

tion imageries (1 km) corresponding to the year 2014 were downloaded. Satellite imagery pertaining to the month of June was used for the computation of C-factor, since during this period onset of monsoon rainfall occurs and the ground is least covered, making the soil susceptible to high degree of potential erosion. Landsat 8 dataset was downloaded from the USGS online data center (http://reverb.echo.nasa.gov/reverb/). CHELSA precipitation imageries were acquired for all the twelve calendar months corresponding to 2014 for derivation of USLE's R-factor and were downloaded from the CHELSA website (http://chelsa-climate.org/). ASTER GDEM was used for the estimation of USLE's LS and P-factor and was downloaded from the National Aeronautics and Space Administration (NASA) online data center (http://reverb.echo.nasa.gov/reverb/). Since, correcting the imageries for atmospheric distortions significantly improves the quality (Huang *et al*. 2002), DN values of the Landsat satellite imagery were converted to radiance, and subsequently to Top of Atmosphere Reflectance units. The transformation of the DN values was carried out using the fast line-of-sight atmospheric analysis of hypercubes (FLAASH) tool available in ENVI 4.8®. In addition, the atmospherically corrected imagery was geometrically rectified based on the appropriate number of well-recognized ground control points (GCPs), acquired from the field visits, topographic maps, and Google Earth imageries. The Landsat OLI, ASTER and CHELSA imageries were transformed to Universal Transverse Mercator Projection (UTM Zone 45, WGS 84), and the area of interest (AOI) was extracted. Geometric rectification of the satellite imagery was carried out in Erdas Imagine 2015® software. Soil map procured from the National Bureau of Soil Survey and Land Utilization Planning (NBSS and LUP) was used for the derivation of textural information, which was further used for the assessment of soil erodibility factor (K). The geomorphic landform features were delineated using the Atlas published under the Rajiv Gandhi National Drinking Water Mission project at 1:50 000 scale by the National Remote Sensing Center (NRSC), Department of Space, Hyderabad. The flowchart of the methodology is presented in Fig. 3.

The vegetation and crop management factor (C) was computed using the vegetation indices computed from the satellite imageries as advocated by Wischmeier and Smith (1978). The USLE model is widely accepted for soil loss estimation for over 35 years. It estimates long-term annual soil loss and guide conservationists on proper cropping, management, and conservation practices. The method is observed as a multiplier of rainfall erosivity (the R factor, which equals the potential energy); this multiplies the resistance of the environment, which comprises K (soil erodibility), SL (the topographical factor), C (plant cover and farming techniques) and P (erosion control practices). The USLE equation is represented as:

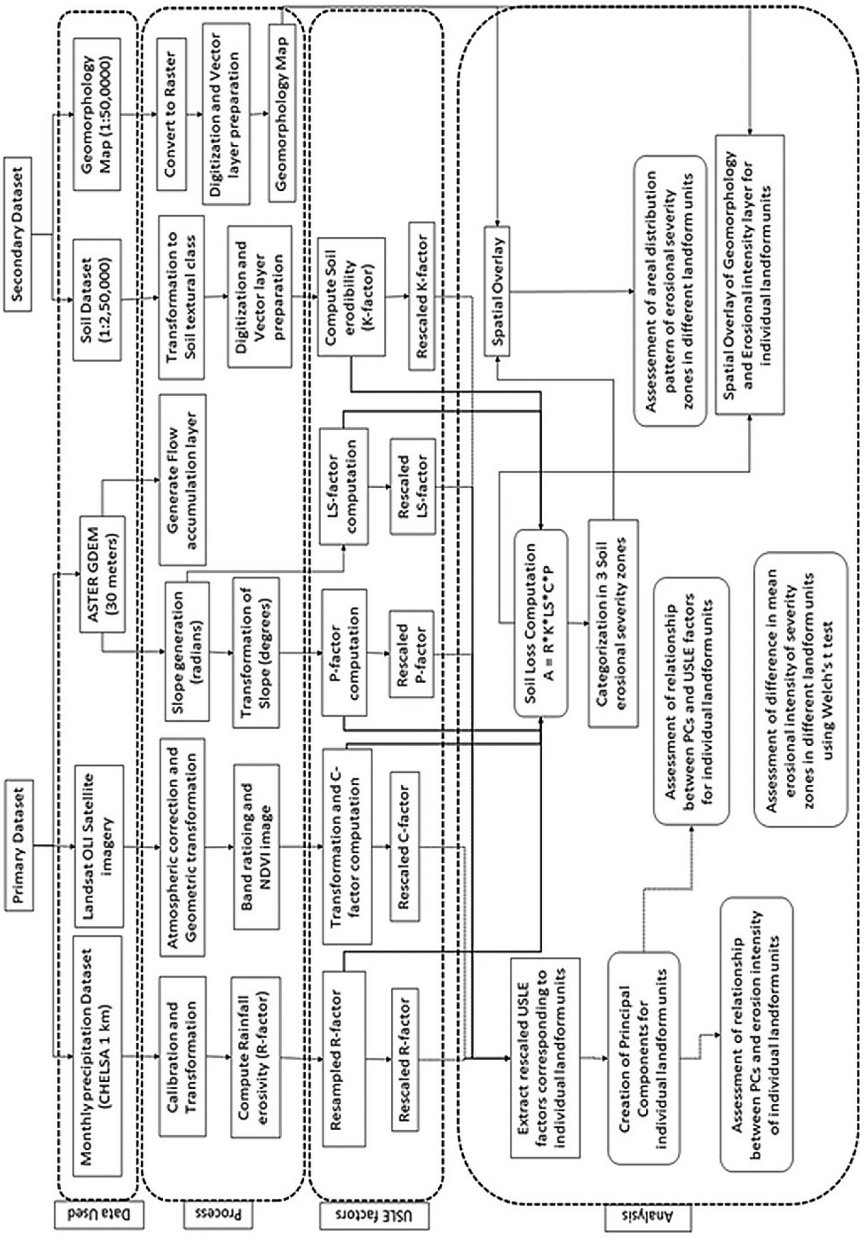

Fig. 3. Flowchart showing the methodological framework

$$A = R \times K \times L \times S \times C \times P \quad (1)$$

where A is the average annual soil loss (tons ha^{-1} year^{-1}); R is the rainfall erosivity (MJmm ha^{-1} hour year); K is the soil erodibility factor (tons ha^{-1}R unit^{-1}); L and S are the topographic factor (dimensionless); C is the cropping management factor (dimensionless), and P is the practice support factor (dimensionless).

Rainfall erosivity factor (R): Most appropriately called the "erosivity index", it is a statistic calculated from the annual summation of rainfall energy in every storm (correlates with raindrop size). This factor corresponds to the potential erosion risk in a given region where sheet erosion appears on a bare plot. In the present investigation, the R-factor for the year 2014 was computed using the following equation:

$$LogR = 1.93 \log \sum \frac{pi^2}{P} - 1.52 \quad (2)$$

where pi is the monthly precipitation; P is the annual precipitation.

Soil erodibility factor (K): The factor quantifies the cohesive, or bonding character of a soil type and its resistance to dislodging and transport due to raindrop impact and overland flow. It largely depends on the organic matter and texture of the soil, its permeability and profile structure. The K-factor values reflect the rate of soil loss per rainfall erosivity index. It can be best obtained from direct measurements on natural runoff plots, since rainfall simulation studies are less accurate, and predictive relationships are least accurate (Kim 2006). The K-factor values corresponding to various soil texture type were derived from Chatterjee *et al*. (2014) and Schwab and Frevert (1981).

Slope and **slope length factor (LS):** Steep slopes produce higher overland flow velocities and, longer slopes accumulate runoff from larger areas. Although they seem opposite in nature, both increase potential rate soil erosion, but in a non-linear manner. Thus, for convenience, length of slope (L) and the degree of slope (S) are frequently lumped into a single term. In the present investigation, the LS-factor is computed using the ArcGIS raster calculator tool (Gelagay and Minale 2016, Mondal *et al*. 2018, Simms *et al*. 2003, Yang and Chapman 2006) using the flow accumulation, and slope layer generated from 30 m ASTER GDEM dataset and, can be represented by the following equation:

$$LS = \left(\frac{flowaccumulation \times cellsize}{22.13}\right)^{0.6} \times \left(\frac{\sin slope \times 0.01745}{0.09}\right)^{1.3} \quad (3)$$

Crop management factor (C): The factor is computed as the ratio of the soil loss from the land cropped under specified conditions to the corresponding loss under tilled, continuous fallow conditions. It is one of the most complicated

USLE factors in terms of computation that integrates the effects of cropping and management practices on the soil erosional intensities. It incorporates the effects of tillage management, crops, seasonal erosivity distribution, and crop rotation. The C-factor values generally range from 0 to 1; where a value of 1 indicates no vegetation cover on the land surface and is treated as exposed bare land, whereas C-factor value near zero (0) indicates very strong cover effects and well-protected soil. Traditionally, the C-factor values corresponding to the different LULC categories are estimated from the plots. However, the approach fails to address the intermittent LULC heterogeneity that persists on the landscape. With the advancement of remote sensing and geographical information system (GIS), various vegetation indices came into existence, for an analysis of the ground cover scenario of the earth's landscape. Normalized difference vegetation index (NDVI) is one of the globally trusted index used for vegetation studies. Here in the present investigation, we used NDVI for derivation of C-factor values using the relationship given by Lin *et al.* (2002). Below listed equations were used for the computation of NDVI and C-factor.

$$NDVI = \frac{NIR - R}{NIR + R} \tag{4}$$

$$C = \left(\frac{1-NDVI}{2}\right)^{1+NDVI} \tag{5}$$

Conservation and support practice factor (P): The factor takes into account specific erosion control practices such as contour tilling or mounding, strip cropping (alternate crops on a given slope established on the contour), and terracing. Its values vary from 1 for bare soil with no erosion control to about 1/10 with tied ridging on a gentle slope. Several researchers suggested that *p*-value is dependent on the slope inclination (Kim 2006, Shin 1999, Wischmeier and Smith 1978), while others put emphasize on the use of farming practices to calculate *p*-value (Stone and Hilborn 2012). In the present investigation, we have computed P-factor based on slope inclination as suggested by Shin (1999).

The estimated average annual soil erosion layer was reclassed under three soil erosional severity zones, i.e. high, medium and low. From the analysis of the soil erosion histogram (Fig. 4), it becomes evident that the dataset is highly skewed. Therefore, for proper representation and categorization of the severity zones, the geometrical interval classification method was used.

The benefit of the geometrical interval classification is that it works reasonably well on the datasets that do not follow normal distribution; in fact, the method was designed to work on the datasets that are heavily skewed. In the next step, spatial overlay operation was performed between the reclassed soil loss layer and the geomorphological landform layer. The overlay operation yielded spatial distribution statistics corresponding to the different soil erosional

severity zones occurring in the individual landform units. The reclassed soil erosion map was used for the assessment of the mean erosion rates in the different severity zones of the various landforms. The raster layers of the soil erosion pertaining to the different landforms were converted to the point layers and, using the Excel ToolPak, Welch's *t*-test for unequal variances and unequal sample size was performed between the different landforms.

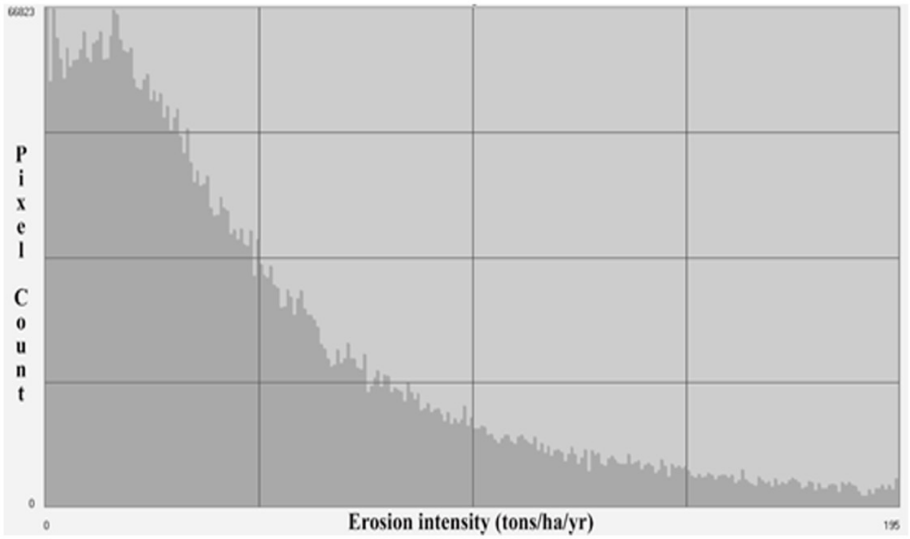

Fig. 4. Histogram of the computed soil erosion intensity

Principal component analysis

Principal components analysis (PCA) is a data transformation technique, which transforms the original data into a new set of data that may better represent the desired information. Often multivariate datasets with large population portray considerable similarity or correlation among them, which results in redundancy of some of the variables. PCA transforms the information contained in the original set of variables into few variables, known as principal components (PCs) in such a manner that the lower order PCs comprise higher information, with decreasing information content in the higher order PCs (Estornell *et al*. 2013). In case of the multispectral raster satellite images, the spectral bands represent the variables, which can be represented in a matrix form as follows:

$$X_{n,b} = \begin{bmatrix} x_{1,1} & \cdots & x_{1,n} \\ \vdots & \ddots & \vdots \\ x_{6,1} & \cdots & x_{6,n} \end{bmatrix}$$

where *n* represents the number of the pixels, and *b* is the number of bands.

Considering each band as a vector, the above matrix can be represented as:

$$X_k = \begin{bmatrix} x_1 \\ x_2 \\ \vdots \\ x_6 \end{bmatrix}$$

where *k* represents the number of bands.

In order to reduce the dimensionality of the original dataset, the eigenvalues of the covariance matrix is computed, and can be represented as:

$$C_{b,b} = \begin{bmatrix} \sigma_{1,1} & \cdots & \sigma_{1,6} \\ \vdots & \ddots & \vdots \\ \sigma_{6,1} & \cdots & \sigma_{6,6} \end{bmatrix}$$

where $\sigma_{i,j}$, denotes the covariance between each pair of bands

$$\sigma_{i,j} = \frac{1}{N-1} \sum_{p=1}^{N} (DN_{p,i} - \mu_i)\,(DN_{p,j} - \mu_j) \tag{6}$$

where $DN_{p,i}$ represents the digital number of a pixel p, in band i, whereas $DN_{p,j}$ is the digital number of a pixel p in the band j, and μ_i and μ_j denote the mean of the *DN* for the bands i and j, respectively.

Using the variance-covariance matrix, eigenvalues (λ) are computed as roots of the equation:

$$det(C - \lambda I) = 0 \tag{7}$$

where *C* and *I* represent the covariance matrix of the bands and diagonal identity matrix, respectively.

The eigenvalues represent the original information of the bands. Using eigenvalues, percent original variance (as explained by different PCs) can be obtained by computing the ratio between each eigenvalue and the sum of all of them. The PCs with minimum variance means that the least information can be discarded. The PCs in a matrix form can then be represented as:

$$Y_6 = \begin{bmatrix} y_1 \\ y_2 \\ \vdots \\ y_6 \end{bmatrix} = \begin{bmatrix} w_{1,1} & \cdots & w_{1,6} \\ \vdots & \ddots & \vdots \\ w_{6,1} & \cdots & w_{6,6} \end{bmatrix} \begin{bmatrix} x_1 \\ x_2 \\ \vdots \\ x_6 \end{bmatrix}$$

where *Y* represents the vector of the PCs, *W* is the transformation matrix, and *X* represents the vector of the original dataset.

The eigenvectors (coefficients of the transformation matrix) can be computed using the vector-matrix equation for each eigenvalue λ_k:

$$(C - \lambda_k I)w_k = 0 \tag{8}$$

where C denotes the covariance matrix, λ_k represents the k eigenvalues (six in the present example), I is the diagonal identity matrix, and w_k is the k eigenvectors.

The PCs were computed from the various USLE parameters considered as different variables for each landform unit. Since the different parameters of USLE have specific units of measurements, before the computation of the PCs, the parameters were transformed into the same scale. The present study comprises assessment of the relationship (i) between the individual PCs and USLE parameters in order to determine the significant USLE parameter(s) and (ii) between the individual PCs and USLE-derived soil erosion model based on the Pearson's correlation coefficients for the respective landform units.

Welch's t-test

It is a non-parametric modification of Student's *t*-test to determine if two sample means are significantly different. Welch's *t*-test is performed between two groups of samples having unequal variance. When two groups have equal sample sizes and variances, Welch's *t*-test tends to give the same result as the Student's *t*-test. However, when sample sizes and variances are unequal, Student's *t*-test is quite unreliable and in such cases, Welch's *t*-test performs better. It can be represented as:

$$t = \frac{\bar{X}1 - \bar{X}2}{\sqrt{\frac{s_1^2}{N_1} + \frac{s_2^2}{N_2}}} \tag{9}$$

where $\bar{X}1$ and $\bar{X}2$ represent the means of groups 1 and 2, s_1^2 and s_2^2 represent the sizes of groups, and N_1 and N_2 are the standard deviation of the two groups, respectively (Seetharaman and Selvaraju 2016, Tang and Dubayah 2017).

RESULTS AND DISCUSSIONS

Spatial distribution of landforms in different severity zones

Table 1 depicts the spatial distribution of landforms under the various soil erosion severity zones. Among the twenty different types of geomorphological units present in the study area, nine represent erosional landforms, five depositional landforms and six denudational/residual landforms, which constitute

87%, 5% and 8% of the area, respectively, thereby indicating that the study area is dominated by the erosional landforms. The four erosional landforms covering more than 10% of the area each are: Plateau Weathered Shallow, Structural Hills, Plateau Weathered Moderate and Plateau Moderately Dissected, which together constitute three-fourth portion of the study area. The other major erosional landforms comprise Valley and Valley Gullied, which constitute 11% of the study area. The depositional and denudational categories each comprise only a single major unit, i.e. Valley Fill Shallow and Pediment Inselberg Complex, respectively, which cover only 10% of the study area.

Table 1. Spatial distribution of the landforms in different severity zones

Landforms	Net Area of	Severity Zone I		Severity Zone II		Severity Zone III	
Name	Landform (hectare)	Area (hectare)	Area (%)	Area (hectare)	Area (%)	Area (hectare)	Area (%)
Erosional landforms							
Structural Hill	35,513.46	15,399.63	43.36	7,401.24	20.84	12,712.59	35.80
Valley	15,017.94	8,358.84	55.66	3,242.70	21.59	3,416.40	22.75
Plateau Weathered Shallow	57,064.50	33,360.39	58.46	15,036.84	26.35	8,667.27	15.19
Plateau Weathered Moderate	35,073.63	19,249.74	54.88	8,117.73	23.14	7,706.16	21.97
Plateau Moderately Dissected	21,275.91	11,084.76	52.10	5,225.85	24.56	4,965.30	23.34
Pediment Moderately Dissected	374.94	208.08	55.50	97.20	25.92	69.66	18.58
Valley Gullied	7,358.76	4,722.84	64.18	1,657.08	22.52	978.84	13.30
Plateau Slightly Dissected	2,771.55	1,421.64	51.29	741.06	26.74	608.85	21.97
Intermontane Valley	249.57	134.37	53.84	50.04	20.05	65.16	26.11
Depositional landforms							
Pediplain Shallow	954.09	551.97	57.85	269.37	28.23	132.75	13.91
Valley Fill Shallow	9,054.81	5,386.14	59.48	2,390.49	26.40	1,278.18	14.12
Piedmont Slope	560.43	269.01	48.00	139.41	24.88	152.01	27.12
Lateritic Plain Moderate	30.60	15.93	52.06	4.50	14.71	10.17	33.24
Flood Plain Shallow	409.41	267.84	65.42	103.23	25.21	38.34	9.36
Denudational landforms							
Pediment Inselberg Complex	10,750.50	5,405.49	50.28	2,124.81	19.76	3,220.20	29.95
Denudated Hill	1,536.03	704.79	45.88	249.93	16.27	581.31	37.84
Residual Hill	1,871.10	920.52	49.20	349.11	18.66	601.47	32.15
Hill Top Weathered	927.00	435.69	47.00	225.27	24.30	266.04	28.70
Inselberg	592.20	287.19	48.50	108.99	18.40	196.02	33.10
Inselberg Complex	44.46	20.52	46.15	11.52	25.91	12.42	27.94

In general, the lowest severity zone alone covers more than 50% of the area under the different landforms, which could be attributed to the dominance of gentle slope in the entire study area. The area covered under the different severity zones is found to decrease from the lower severity zone to the higher severity zone in case of erosional and depositional landforms. In contrast, the various denudational landforms together exhibit larger area in the highest severity zone as compared to the moderate severity zone.

Analysis of the mean and CV of the annual soil erosion values for different landforms

Table 2 shows the mean and coefficient of variation (CV) of the soil erosion values corresponding to the different erosional, depositional and denudational landforms. The soil erosion computed for the different pixels have been categorized into three severity zones viz. severity zone 1, 2 and 3 in order of increasing severity. Comparative analysis of the mean and CV values reveals drastic increase in the mean values from the lower severity zone to the higher severity zone, successively. In fact, the mean erosional estimates in the lowest severity zone are quite small with the values less than 1, which increases by more than one hundred times in the highest severity zone, indicating significant rise in soil erosion. Occurrence of very small mean values with relatively higher standard deviation results in very high CV values in the lowest severity zone.

Table 2. Mean and CV of the annual soil erosion values of the landforms corresponding to the different severity zones

Landforms	Severity Zone 1 (< 9.89 tons/ha/yr)			Severity Zone 2 (9.89–48,026 tons/ha/yr)			Severity Zone 3 (> 48,026 tons/ha/yr)		
	Mean	Std. dev	CV	Mean	Std. dev	CV	Mean	Std. dev	CV
Erosional landforms									
Structural Hill	0.61	1.95	319.61	27.58	10.83	39.25	126.33	54.47	43.12
Valley	0.66	1.94	294.90	27.26	10.81	39.64	109.36	51.59	47.17
Plateau Weathered Shallow	0.77	2.13	274.60	26.10	10.54	40.41	99.01	48.88	49.37
Plateau Weathered Moderate	0.59	1.88	320.49	27.75	10.73	38.68	97.34	44.75	45.97
Plateau Moderately Dissected	0.68	2.03	298.76	27.13	10.71	39.50	104.29	49.17	47.15
Pediment Moderately Dissected	0.72	2.09	288.95	26.80	10.68	39.86	88.04	39.79	45.20
Valley Gullied	0.75	2.04	273.08	25.52	10.58	41.44	107.17	53.95	50.35
Plateau Slightly Dissected	0.63	1.96	309.03	27.27	10.60	38.88	100.94	48.46	48.01

Intermontane Valley	0.37	1.52	405.99	29.17	11.33	38.85	107.08	50.26	46.93
Depositional landforms									
Pediplain Shallow	0.80	2.18	272.43	26.13	10.50	40.20	101.50	49.90	49.16
Valley Fill Shallow	0.89	2.23	252.07	25.30	10.42	41.20	106.04	52.88	49.87
Piedmont Slope	0.76	2.14	281.16	26.95	10.62	39.41	117.79	53.51	45.43
Lateritic Plain Moderate	0.24	1.37	560.68	25.96	10.22	39.38	118.41	49.61	41.90
Flood Plain Shallow	0.93	2.27	244.22	25.12	10.44	41.56	93.44	47.71	51.05
Residual landforms									
Pediment Inselberg Complex	0.47	1.71	362.47	28.75	10.76	37.43	111.37	50.88	45.68
Denudational Hill	0.49	1.75	354.24	27.06	10.96	40.50	142.37	54.93	38.58
Residual Hill	0.47	1.72	366.73	27.90	10.75	38.53	125.28	55.12	44.00
Hill Top Weathered	0.50	1.78	357.33	28.04	10.73	38.27	111.41	51.42	46.15
Inselberg	0.43	1.62	379.88	28.77	10.96	38.12	119.34	53.55	44.87
Inselberg Complex	0.96	2.50	260.73	27.43	10.27	37.45	115.65	52.30	45.23

On the one hand, the mean erosion values are found to be higher than the standard deviation in the two higher severity zones that results in smaller CV values. The CV values in the moderate and highest severity zones, i.e. in severity zones 2 and 3, respectively, are found to be nearly the same. The CV values represent the heterogeneity of the pixel wise erosional estimates within a particular severity zone. Among the different landforms, the three types of hills viz. Structural Hill, Denudational Hill and Residual Hill depict conspicuously higher mean erosion as compared to the other landforms. In the highest severity zone, Denudational Hill depicts the highest mean erosion, whereas the other two types of hill landforms exhibit nearly the same mean soil erosion. On the other hand, five types of erosional landforms, which exhibit significantly small mean erosion, are Plateau Weathered Shallow, Plateau Weathered Moderate, Pediment Moderately Dissected, Plateau Slightly Dissected and Flood Plain Shallow.

Relationship between soil erosion and principal components (PCs)

As mentioned earlier, USLE determines the cumulative effect of the different influencing factors such as rainfall erosivity, soil erodibility, slope length, crop management factor and conservation practices, which may exhibit considerable correlation between them. The cumulative effect of the different influencing factors can also be represented by the principal components determined

from these factors, which integrate the variance associated with the different influencing factors. The first principal component (PC1) comprises the maximum variance extracted from the original variables. The next higher order principal component (PC2) is computed by the linear combination of the remaining variance associated with the different influencing factors, and so on. Depending upon the nature and magnitude of the correlation between the different influencing factors, each PC would account for the different amount of contributions from the various influencing factors. As a result, each principal component could exhibit different amount and nature of correlation with the various influencing parameters used in USLE. Table 3 depicts the eigenvalues associated with the different PCs.

Table 3. Eigenvalue distribution among different PCs

Landforms	Percent of eigenvalues				
	PC1	PC2	PC3	PC4	PC5
Erosional landforms					
Structural Hill	50.34	35.95	7.78	5.76	0.17
Valley	44.44	26.95	16.37	12.00	0.24
Plateau Weathered Shallow	38.19	30.14	20.83	10.76	0.08
Plateau Weathered Moderate	37.77	30.40	18.20	13.58	0.05
Plateau Moderately Dissected	40.21	35.36	15.31	9.03	0.09
Pediment Moderately Dissected	77.77	12.44	7.94	1.83	0.02
Valley Gullied	47.71	29.44	16.85	5.53	0.47
Plateau Slightly Dissected	64.35	24.49	7.34	3.71	0.11
Intermontane Valley	59.75	38.67	1.31	0.28	0.00
Depositional landforms					
Pediplain Shallow	49.44	39.25	7.08	4.17	0.06
Valley Fill Shallow	41.95	29.49	20.93	7.38	0.24
Piedmont Slope	75.56	14.02	5.86	4.32	0.23
Lateritic Plain Moderate	74.17	25.74	0.09	0.00	0.00
Flood Plain Shallow	65.33	31.37	2.70	0.60	0.00
Denudational landforms					
Pediment Inselberg Complex	47.29	25.93	15.02	11.69	0.07
Denudated Hill	64.54	21.78	9.67	3.92	0.10
Residual Hill	51.52	22.72	16.53	9.17	0.07
Hill Top Weathered	49.55	32.90	11.05	6.43	0.06
Inselberg	56.40	21.15	15.61	6.75	0.09
Inselberg Complex	74.05	17.08	5.74	3.05	0.08

In the present study, correlation coefficients have been determined between the USLE-derived soil erosion layer and individual principal components for each geomorphological landform (Table 4). The correlation coefficients were found to be significant at $p < 0.05$.

Table 4. Relationship (coefficient of correlation) between soil erosion and principal components

Erosional landforms					
Landforms	Coefficient of correlation (R)				
	PC1	PC2	PC3	PC4	PC5
Structural Hills	0.24	0.18	0.41	-0.03	-0.53
Plateau Weathered Shallow	0.14	0.12	0.16	0.08	-0.64
Plateau Weathered Moderate	0.03	0.04	0.18	0.05	-0.72
Plateau Moderately Dissected	0.15	0.13	0.29	0.00	-0.59
Pediment Moderately Dissected	-0.10	0.13	0.18	-0.04	-0.80
Valley Gullied	0.02	0.01	0.12	0.06	-0.58
Plateau Slightly Dissected	0.12	0.12	0.25	-0.04	-0.57
Intermontane Valley	0.21	0.20	0.15	-0.16	-0.62
Valley	0.07	0.12	0.17	0.06	-0.51
Depositional landforms					
Pediplain Shallow	0.32	0.30	0.23	-0.13	-0.84
Valley Fill Shallow	0.15	0.09	0.17	-0.03	-0.51
Piedmont Slope	0.47	0.37	0.33	0.20	-0.62
Lateritic Plain Moderate	0.22	0.22	0.24	-0.22	-0.83
Flood Plain Shallow	-0.01	-0.03	0.18	-0.05	-0.49
Residual landforms					
Pediment Inselberg Complex	0.15	0.09	0.28	0.01	-0.69
Denudated Hill	0.26	0.24	0.46	0.29	-0.68
Residual Hill	0.25	0.20	0.37	-0.01	-0.69
Hill Top Weathered	0.29	0.18	0.35	-0.09	-0.66
Inselberg	0.22	0.16	0.32	0.09	-0.58
Inselberg Complex	0.26	0.16	0.37	0.09	-0.62

The first three PCs, i.e. PC1, PC2, PC3 exhibit positive but weak correlation with the USLE-derived soil erosion layer for the different landform units with few exceptions, in which the correlation is found to be negative. PC4 shows both positive and negative correlation, however, with relatively much smaller magnitude (Table 3). However, significantly, the highest order PC, i.e. PC5 is found to be strongly correlated with the erosion values although the nature of correlation is negative. Among the different landform units, one single erosional landform viz. Pediment Moderately Dissected and two depositional landforms, i.e. Pediplain Shallow and Laterite Plain Moderate exhibit correlation coefficients of greater than -0.8 with PC5. In case of the remaining landform units, the correlation coefficients between PC5 and soil erosion are found to range between -0.49 and -0.72. Among the different parameters of USLE, LS factor is found to exhibit significantly strong but negative correlation with PC5, with the values of correlation coefficients ranging between -0.90 and -0.99 in the different landform units (Table 5). These observations ascertain dominant role of LS factor in inducing soil erosion in the study area.

Table 5. Coefficient of correlation between PC5 and USLE factors

	R-factor	LS-factor	C-factor	P-factor	K-factor
Erosional landforms					
Structural Hill	0.01	**-0.98**	0.01	-0.02	0.01
Valley	0.02	**-0.99**	0.00	0.02	-0.01
Plateau Weathered Shallow	-0.01	**-0.97**	-0.06	0.06	-0.03
Plateau Weathered Moderate	0.01	**-0.94**	-0.05	0.18	-0.07
Plateau Moderately Dissected	0.02	**-0.97**	-0.05	0.11	-0.03
Pediment Moderately Dissected	-0.02	**-0.95**	-0.11	0.24	-0.10
Valley Gullied	0.00	**-0.99**	-0.01	0.04	-0.03
Plateau Slightly Dissected	0.05	**-0.98**	-0.01	0.12	-0.05
Intermontane Valley	0.01	**-0.98**	0.02	-0.10	0.00
Depositional landforms					
Pediplain Shallow	0.03	**-0.90**	-0.03	0.02	0.00
Valley Fill Shallow	0.03	**-0.99**	0.00	-0.01	0.01
Piedmont Slope	-0.15	**-0.98**	0.14	-0.13	-0.02
Lateritic Plain Moderate	0.02	**-0.94**	-0.08	0.21	0.00
Flood Plain Shallow	0.00	**-0.99**	-0.08	0.06	0.00
Denudational landforms					
Pediment Inselberg Complex	0.03	**-0.94**	-0.09	0.18	-0.01
Denudated Hill	-0.17	**-0.96**	-0.12	0.06	-0.08
Residual Hill	-0.02	**-0.94**	-0.09	0.06	-0.08
Hill Top Weathered	0.01	**-0.94**	-0.02	0.10	-0.05
Inselberg	-0.01	**-0.95**	-0.06	0.18	-0.03
Inselberg Complex	-0.01	**-0.93**	0.03	0.27	-0.16

Welch's *t*-test was performed in order to determine the difference in the erosion estimates between the different geomorphological landforms. Out of the 170 possible pairs of the landform units, 148 pairs (87%) are found to be significantly different at $p < 0.01$, whereas 22 pairs of landform units (13%) exhibit similar erosion rates. Among the different landform units, Structural Hill exhibits significantly different erosion estimate with the maximum landform units.

CONCLUSIONS

The main objective of the present investigation was to evaluate the role of the various geomorphological landforms on the occurrence of soil erosion. The study was conducted by considering three broad categories of landforms, i.e. erosional, denudational and depositional present in the study area. We have employed the standard USLE to estimate the soil loss in each landform unit. The erosional severity of each landform unit was categorized into three types such as low, medium and high, in order to determine the spatial extent of the respective landforms falling under the different severity zones. Further, in order to deter-

mine the combined influence of all the five USLE factors on the soil erosion in the various landform units, we determined principal components from the USLE factors and subsequently, performed Pearson's correlation between each principal component and soil erosion. Subsequently, in order to determine the most influential factor of USLE, we determined correlation coefficients between PC5 and respective influencing factors of USLE for the individual landform units. Welch's *t*-test was implemented to determine the difference in the erosional severity between the different landform units. The salient findings from the investigation are highlighted below.

1. The correlation analysis revealed the occurrence of highest and negative correlation of the erosion estimate with PC5.

2. LS factor is found to be pre-dominant among the various factors in USLE-derived soil loss determined for the different landforms.

3. Welch's *t*-test analysis ascertained that the majority of the landform units are significantly different from each other in terms of their role in inducing soil erosion. There exists large difference between the landform units belonging to different broad landform categories, i.e. erosional, denudational and depositional. Structural Hill exhibits significantly different erosion estimate with the maximum landform units.

4. These observations ascertain that the landform units can be considered as distinct spatial units, for the characterization of the pattern and severity of soil erosion.

REFERENCES

[1] Abdel Rahman, M.A.E., Shalaby, A., Essa, E.F., 2018. *Quantitative Land Evaluation Based on Fuzzy-Multi-Criteria Spatial Model for Sustainable Land-Use Planning*. Modeling Earth Systems and Environment, 4(4): 1341–1353. https://doi.org/10.1007/s40808-018-0478-1.

[2] Champagnac, J.-D., Molnar, P., Sue, C., Herman, F., 2012. *Tectonics, Climate, and Mountain Topography*. Journal of Geophysical Research: Solid Earth, 117(B2). https://doi.org/10.1029/2011JB008348.

[3] Chatterjee, S., Krishna, A.P., Sharma, A.P., 2014. *Geospatial Assessment of Soil Erosion Vulnerability at Watershed Level in Some Sections of the Upper Subarnarekha River Basin, Jharkhand, India*. Environmental Earth Sciences, 71(1): 357–374. https://doi.org/10.1007/s12665-013-2439-3.

[4] Conoscenti, C., Di Maggio, C., Rotigliano, E., 2008. *Soil erosion Susceptibility Assessment and Validation Using a Geostatistical Multivariate Approach: A Test in Southern Sicily*. Natural Hazards, 46(3): 287–305. https://doi.org/10.1007/s11069-007-9188-0.

[5] Council, N.R., 2010. *Landscapes on the Edge: New Horizons for Research on Earth's Surface*. Washington, DC: The National Academies Press.

[6] Estornell, J., Marti Gavilá, J., Sebastiá, M.T., Mengual, J., 2013. *Principal Component Analysis Applied to Remote Sensing*. Modelling in Science Education and Learning, 6(2): 83–89. https://doi.org/10.4995/msel.2013.1905.

[7] Gelagay, H.S., Minale, A.S., 2016. *Soil loss Estimation Using GIS and Remote Sensing Techniques: A Case of Koga Watershed, Northwestern Ethiopia*. International Soil and Water Conservation Research, 4(2): 126–136. https://doi.org/10.1016/j.iswcr.2016.01.002.

[8] Huang, C., Wylie, B.K., Yang, L., Homer, C.G., Zylstra, G., 2002. *Derivation of a Tasselled Cap Transformation Based on Landsat 7 at Satellite Reflectance*. International Journal of Remote Sensing, 23(8): 1741–1748. https://doi.org/10.1080/01431160110106113.
[9] Kim, H.S., 2006. *Soil Erosion Modeling Using RUSLE and GIS on the Imha Watershed, South Korea*: Colorado State University.
[10] Lin, C.Y., Lin, W.T., Chou, W.C., 2002. *Soil Erosion Prediction and Sediment Yield Estimation: The Taiwan Experience*. Soil and Tillage Research, 68(2): 143–152.
[11] Mainuri, Z.G., Owino, J.O., 2014. *Linking Landforms and Land Use to Land Degradation in the Middle River Njoro Watershed*. International Soil and Water Conservation Research, 2(2): 1–10. doi: https://doi.org/10.1016/S2095-6339(15)30001-0.
[12] Marston, R.A., 2010. *Geomorphology and Vegetation on Hillslopes: Interactions, Dependencies, and Feedback Loops*. Geomorphology, 116(3): 206–217. https://doi.org/10.1016/j.geomorph.2009.09.028.
[13] McGrath, G., Paik, K., Hinz, C. 2011. *Complex Landscapes from Simple Ecohydrological Feedbacks*. Paper presented at the MODSIM 2011, Proceedings of the 19th International Congress on Modelling and Simulation, Australia.
[14] Mondal, A., Khare, D., Kundu, S., 2018. *A Comparative Study of Soil Erosion Modelling by MMF, USLE and RUSLE*. Geocarto International, 33(1): 89–103. https://doi.org/10.1080/10106049.2016.1232313.
[15] Morgan, R.P.C., Nearing, M., 2016. *Handbook of Erosion Modelling*: Wiley.
[16] Morgan, R.P.C., Rickson, R.J., 2003. *Slope Stabilization and Erosion Control: A Bioengineering Approach*: Taylor & Francis.
[17] Mukherjee, S., Mukherjee, S., Garg, R.D., Bhardwaj, A., Raju, P.L.N., 2013. *Evaluation of Topographic Index in Relation to Terrain Roughness and DEM Grid Spacing*. Journal of Earth System Science, 122(3): 869–886. https://doi.org/10.1007/s12040-013-0292-0.
[18] Patel, N., Kathwas, A.K., 2012. *Assessment of Spatio-Temporal Dynamics of Soil Erosional Severity Through Geoinformatics AU-Patel, Nilanchal*. Geocarto International, 27(1): 3–16. https://doi.org/10.1080/10106049.2011.614359.
[19] Patton, N.R., Lohse, K.A., Godsey, S.E., Crosby, B.T., Seyfried, M.S., 2018. *Predicting Soil Thickness on Soil Mantled Hillslopes*. Nature Communications, 9(3329). https://doi.org/10.1038/s41467-018-05743-y.
[20] Pelletier, J.D., Barron-Gafford, G.A., Breshears, D.D., Brooks, P.D., Chorover, J., Durcik, M., ... Troch, P.A., 2013. *Coevolution of Nonlinear Trends in Vegetation, Soils, and Topography with Elevation and Slope Aspect: A Case Study in the Sky Islands of Southern Arizona*. Journal of Geophysical Research: Earth Surface, 118(2): 741–758. https://doi.org/10.1002/jgrf.20046.
[21] Pennock, D.J., 2003. *Terrain Attributes, Landform Segmentation, and Soil Redistribution*. Soil and Tillage Research, 69(1): 15–26. https://doi.org/10.1016/S0167-1987(02)00125-3.
[22] Saco, P., Willgoose, G., Hancock, G., 2007. *Eco-Geomorphology of Banded Vegetation Patterns in Arid and Semi-Arid Regions*. Hydrology and Earth System Sciences, 11. https://doi.org/10.5194/hess-11-1717-2007.
[23] Schoonover, J.E., Crim, J.F., 2015. *An Introduction to Soil Concepts and the Role of Soils in Watershed Management*. Journal of Contemporary Water Research & Education, 154(1): 21–47. https://doi.org/10.1111/j.1936-704X.2015.03186.x.
[24] Schwab, G.O., Frevert, R.K., 1981. *Soil and Water Conservation Engineering*: Wiley.
[25] Seetharaman, D.K., Selvaraju, S., 2016. *Statistical Tests of Hypothesis-Based Color Image Retrieval*. Journal of Data Analysis and Information Processing, 4: 90–99. https://doi.org/10.4236/jdaip.2016.42008.
[26] Segundo Métay, I.G., Bocco, G., Velázquez, A., Gajewski, K., 2017. *On the Relationship Between Landforms and Land Use in Tropical Dry Developing Countries. A GIS and Multivariate Statistical Approach*. Investigaciones Geográficas, Boletín del Instituto de Geografía, 93: 3–19. https://doi.org/10.14350/rig.56438.

[27] Shin, G.J. (1999). *The Analysis of Soil Erosion Analysis in Watershed Using GIS.* Gang-won National University.
[28] Simms, A.D., Woodroffe, C.D., Jones, B.G., 2003, July 14–17. *Application of RUSLE for Erosion Management in a Coastal Catchment, Southern NSW.* Paper presented at the Proceedings of the International Congress on Modeling and Simulation: Integrative Modeling of Biophysical, Social and Economic Systems for Resource Management Solutions, Townsville, Australia.
[29] Stone, R.P., Hilborn, D., 2012. *Universal Soil Loss Equation (USLE) Factsheets.* Ontario: Queen's Printer.
[30] Tang, H., Dubayah, R., 2017. *Light-Driven Growth in Amazon Evergreen Forests Explained by Seasonal Variations of Vertical Canopy Structure*. Procedings of the National Academy of Sciences of the USA, 114(10): 2640–2644. https://doi.org/10.1073/pnas.1616943114.
[31] Whipple, K.X., 2009. *The Influence of Climate on the Tectonic Evolution of Mountain Belts*. Nature Geoscience, 2: 97. https://doi.org/10.1038/ngeo413.
[32] Wischmeier, W.H., Smith, D.D., 1978. *Predicting Rainfall Erosion Losses – a Guide to Conservation Planning.* Hyattsville, Maryland: USDA, Science and Education Administration.
[33] Yang, X., Chapman, G., 2006. *Soil Erosion Modelling for NSW Coastal Catchments Using RUSLE in a GIS Environment.* Paper presented at the Geoinformatics 2006: GNSS and Integrated Geospatial Applications.